Received: 8 February 2023 | Revised: 28 March 2023 | Accepted: 19 April 2023

DOI: 10.1002/prot.26507

RESEARCH ARTICLE

PROTEINS WILEY

Key substrate recognition residues in the active site of cystathionine beta-synthase from *Toxoplasma gondii*

Carolina Conter[1] | Filippo Favretto[1] | Paola Dominici[1] | Luis Alfonso Martinez-Cruz[2] | Alessandra Astegno[1]

[1]Department of Biotechnology, University of Verona, Verona, Italy

[2]Center for Cooperative Research in Biosciences (CIC bioGUNE), Basque Research and Technology Alliance (BRTA), Derio, Spain

Correspondence
Alessandra Astegno, Department of Biotechnology, University of Verona, Strada Le Grazie 15, 37134 Verona, Italy.
Email: alessandra.astegno@univr.it

Funding information
Italian Minister of University and Research, Grant/Award Number: FUR2022; Italian MIUR-PRIN 2017, Grant/Award Number: 2017ZBBYNC

Abstract

Cystathionine β-synthase (CBS) catalyzes the condensation of L-serine and L-homocysteine to give L-cystathionine in the transsulfuration pathway. Recently, a few *O*-acetylserine (L-OAS)-dependent CBSs (OCBSs) have been found in bacteria that can exclusively function with L-OAS. CBS from *Toxoplasma gondii* (*Tg*CBS) can efficiently use both L-serine and L-OAS to form L-cystathionine. In this work, a series of site-specific variants substituting S84, Y160, and Y246 with hydrophobic residues found at the same positions in OCBSs was generated to explore the roles of the hydroxyl moieties of these residues as determinants of L-serine/L-OAS preference in *Tg*CBS. We found that the S84A/Y160F/Y246V triple mutant behaved like an OCBS in terms of both substrate requirements, showing β-replacement activity only with L-OAS, and pH optimum, which is decreased by ∼1 pH unit. Formation of a stable aminoacrylate upon reaction with L-serine is prevented by the triple mutation, indicating the importance of the H-bonds between the hydroxyl groups of Y160, Y246, and S84 with L-serine in formation of the intermediate. Analysis of the independent effect of each mutation on *Tg*CBS activity and investigation of the protein–aminoacrylate complex structure allowed for the conclusion that the hydroxyl group of Y246 has a major, but not exclusive, role in controlling the L-serine preference by efficiently stabilizing its leaving group. These studies demonstrate that differences in substrate specificity of CBSs are controlled by natural variations in as few as three residue positions. A better understanding of substrate specificity in *Tg*CBS will facilitate the design of new antimicrobial compounds.

KEYWORDS
cystathionine β-synthase, enzyme kinetics, mutagenesis, substrate specificity, *Toxoplasma gondii*

1 | INTRODUCTION

Cystathionine β-synthase (CBS, EC 4.2.1.22) is a pyridoxal 5′-phosphate (PLP) dependent enzyme that works in the transsulfuration pathway to produce L-cysteine (L-Cys). The enzyme catalyzes the β-replacement of the hydroxyl group of L-serine (L-Ser) by L-homocysteine (L-Hcys) to yield L-cystathionine (L-Cth) and water through the formation of an aminoacrylate intermediate (ping-pong reaction) (Figure 1). The resulting L-Cth is further converted to L-Cys, ammonia, and α-ketobutyric acid by cystathionine γ-lyase (CGL, EC

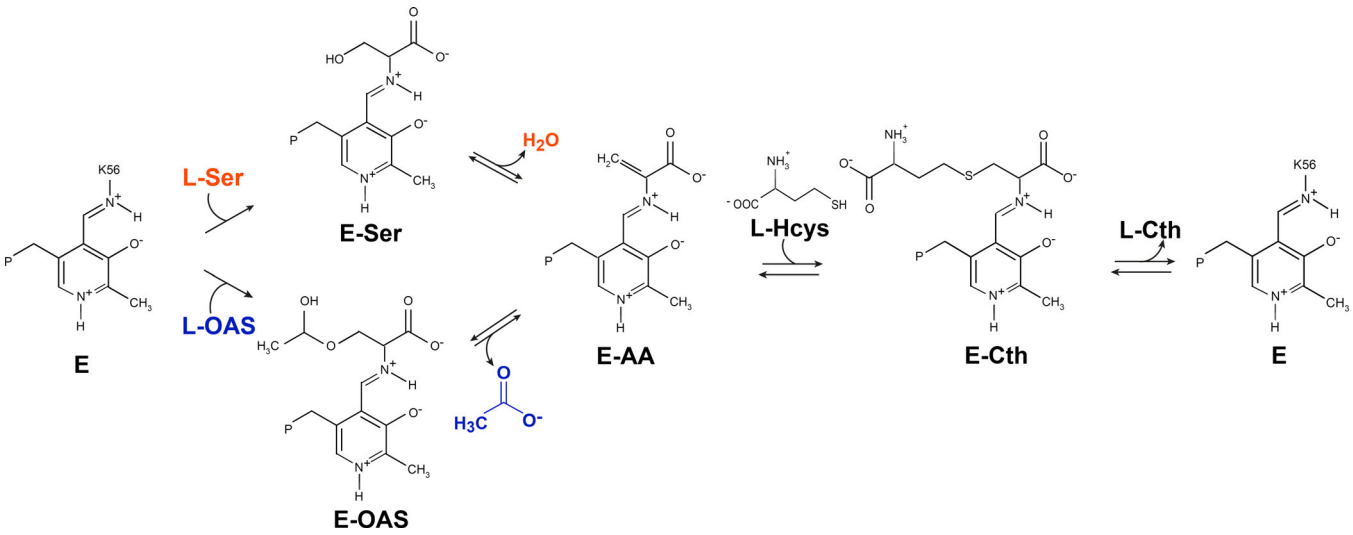

FIGURE 1 Reaction mechanism of CBS. E, E-Ser, E-OAS, E-AA and E-Cth refer to the internal aldimine, the external aldimine of L-Ser (or L-OAS), the aminoacrylate intermediate and the external aldimine of L-Cth, respectively.

4.4.1.1). CBS can also catalyze alternative L-Cys- and L-Hcys-dependent reactions to release hydrogen sulfide (H_2S), an important signaling molecule that is involved in modulating cell function.

CBS is a modular enzyme that, depending on the organism, adopts different domain architectures.[1] Mammals possess the most complex version of the enzyme in which the N- and C-terminal domains bind heme and the allosteric modulator *S*-adenosyl-L-methionine (AdoMet), respectively. The C-terminal domain includes a pair of CBS domains, named the Bateman module, which prevents the access of substrates into the catalytic site by acting as a cap. The binding of AdoMet to this C-terminal region causes a rotation of the CBS domains and triggers clashes with the structural elements configuring the entrance of the catalytic core. Such steric hindrance promotes the displacement of the Bateman module from the catalytic cavity and alleviates the cap effect by increasing substrate access and enabling the enzyme to shift from a basal to an activated state.[2–5] In insects CBSs, like those from the fruit fly[6] and honeybee,[7] the Bateman module associates with the same area of a complementary subunit, forming a disk-shaped assembly known as "CBS module." This CBS module remains distant from the entry of the catalytic cavity and contributes to maintaining the enzyme in a constitutively activated state. In contrast, most CBSs from bacteria have a simpler domain architecture in which both the heme and the C-terminal Bateman domains are absent. Recently, some CBSs, referred to as *O*-acetylserine dependent CBSs (OCBSs), have been found in bacteria.[8,9] These enzymes not only lack the N-terminal heme-binding domain and the C-terminal Bateman regulatory domain, but also do not need AdoMet for their activation and exclusively function with L-OAS, thus significantly differing from CBSs of higher organisms. In particular, the ability of bacteria OCBSs to use L-OAS as substrate might be related to specific functional constraints that are required for the survivability of microorganisms. However, the regulatory aspects of the different CBS substrate requirements are still poorly understood. It has been speculated that the difference in some residues close to the active site in CBS and OCBS can affect the ability of the enzyme to process L-OAS or L-Ser.[8,9] Three residues, Ser82, Tyr158, and Tyr248 (residue number according to the conventional yeast CBS), were assumed to be the determinant of this substrate specificity, which differ from OCBS where they are replaced by Ala74, Phe147, and Val226, respectively (residue numbers refer to *H. pylori* OCBS).[8]

We recently showed that CBS from *Toxoplasma gondii* (*Tg*CBS) can use both L-Ser and L-OAS to give L-Cth and is unresponsive to AdoMet, likely linking its catalytic ability to the OCBS enzymes.[10–12] However, *Tg*CBS possesses higher sequence similarity to CBS than OCBS as it contains a C-terminal Bateman module and, with respect to the above-mentioned active site fingerprint, the residues of canonical CBS (Ser, Tyr, and Tyr). The particular structural features of *Tg*CBS were recently unraveled from the crystal structure of the enzyme.[12] We found that, as expected, each protomer includes two independent domains, corresponding to an N-terminal catalytic core and a C-terminal Bateman module, which are connected by a long, partially helical linker that maintains tight interactions with both modules (Figure S1). Interestingly, the structure showed that the Bateman module lacks important amino acid residues that are needed to stabilize AdoMet within its two main cavities, thus explaining why *Tg*CBS does not bind and is not activated by this allosteric effector. Furthermore, structural and biophysical data also suggest that *Tg*CBS exists in a sole basket-like dimeric conformation which is similar to that so far found only in the basal state of the human enzyme.[2] In *Tg*CBS, however, the occlusive effect observed in the human enzyme is released by a slight approach of the Bateman module toward the central cleft of the dimer, giving higher space and mobility to the structural elements that configure the entrance of the catalytic cavity, and consequently, the access of substrates.

In the present work, in order to understand the specific features that allow *Tg*CBS to efficiently process L-OAS and L-Ser and whether

the above-mentioned fingerprint residues are important for substrate specificity, we chose Ser84, Tyr160, and Tyr246 for a mutagenesis approach to simulate the substrate-binding site of OCBS. Single-residue substitution mutants (S84A, Y160F, and Y246V) and one triple mutant (S84A/Y160F/Y246V) were constructed and characterized. The detailed kinetic and spectroscopic analysis of the recombinant enzymes in combination with a structural inspection of the active site of *Tg*CBS revealed that the three residues are critical in L-Ser/L-OAS recognition, thus demonstrating that differences in substrate specificity of CBSs are controlled by natural variations in as few as three residue positions.

Investigation of the elements that allow enzymes to control the substrate preference might have important consequences for the development of therapeutics and antimicrobial compounds.

2 | MATERIALS AND METHODS

2.1 | Protein production

*Tg*CBS was expressed in *Escherichia coli* Rosetta (DE3) and purified as previously described.[10] The site-specific mutants were generated by mutagenesis of the pET21a-*Tg*CBS construct, using the QuikChange® site-directed mutagenesis kit (Agilent Technologies). The primers used for all mutations are listed in Table S1. The verified plasmids for the mutated forms of *Tg*CBS were transformed into *E. coli* Rosetta (DE3) host cells and the corresponding proteins were purified as for the wild-type enzyme.[10] The expression levels of all of the *Tg*CBS mutants varied from 60 to 80 mg/L in LB medium. The purity of enzymes was confirmed by SDS-PAGE. The PLP content was measured by releasing the cofactor in 0.1 M NaOH and monitoring absorbance at 388 nm ($\epsilon_{388} = 6600\ M^{-1}\ cm^{-1}$).[13]

The oligomeric state of *Tg*CBS variants was analyzed via gel filtration (GE Healthcare Superdex 200 10/300 GL column) in 20 mM sodium phosphate buffer pH 8.5, 150 mM NaCl and 0.1 mM DTT. A high molecular weight gel filtration calibration kit (GE Healthcare) was employed to generate a calibration curve, following protocols in.[14,15]

2.2 | Spectroscopic measurements

Absorption spectra were recorded on a Jasco V-750 spectrophotometer in a buffer containing 20 mM sodium phosphate pH 8.5 at 25°C using a protein concentration of 12 μM.[10,11] CD spectra were recorded on a Jasco J-1500 CD spectropolarimeter equipped with a Peltier-type temperature controller as previously described.[16,17] Briefly, near UV–Vis (250–600 nm) spectra of 1 mg/mL *Tg*CBS variants were recorded in 1-cm path length quartz cuvette at a scan speed of 50 nm/min. Far-UV (200–250 nm) spectra of 0.2 mg/mL enzyme variants were recorded using a 0.1 cm path length quartz cuvette. A minimum of three accumulations were made for each scan, which were averaged and corrected for the blank solution of the corresponding buffer.

Thermal unfolding was monitored by recording ellipticity at 222 nm between 20 and 90°C (scan rate 1.5°C/min) using 0.1 cm path length quartz cuvettes and protein concentration of 0.2 mg/mL. All CD measurements were carried out in 20 mM sodium phosphate pH 8 or 8.5 at 25°C.[18–20]

2.3 | High-performance liquid chromatography

High-performance liquid chromatography (HPLC) analysis was performed on a Jasco LC-4000 HPLC system with a FP-4020 fluorescence detector as previously reported.[10] Briefly, the production of L-Cth was analyzed by incubating for 2 h at 37°C the *Tg*CBS variants (5 μM) with 1 mM L-Ser (or L-OAS) and 0.8 mM L-Hcys. Upon removal of the enzyme by centrifugation (Vivaspin Turbo centrifugal concentrator, Sartorius), the sample solutions (120 μL) were mixed with the ortho-phthaldialdehyde (OPA) derivatization reagent to a 180 μL final volume using the autosampler. After a 2-min reaction at 4°C, 10 μL of the mixture was injected onto a C-18 RP column (Agilent Poroshell 120 HPH RP-C18, 4 μm, 4.6 × 250 mm). The derivatized products were eluted at a flow rate of 1 mL/min at 40°C using a gradient elution with buffers A (80% 0.1 M sodium acetate pH 4.75 and 20% methanol) and B (20% 0.1 M sodium acetate pH 4.75 and 80% methanol) as described previously.[10,21] Excitation of the fluorescence detector was set at 340 nm and emission at 450 nm.

2.4 | Enzyme assays

CBS canonical activity utilizing L-Ser (or L-OAS) and L-Hcys was measured by applying the continuous cystathionine β-lyase (CBL) and lactate-dehydrogenase (LDH) coupled-coupled assay as previously described[22] with the following modifications. The coupling enzymes were recombinant CBL from *E. coli*, which is produced in our laboratory, and commercial LDH from bovine heart. Enzyme activity was measured at 37°C in a final volume of 200 μL using a Jasco V-750 spectrophotometer. The reaction mixture contained 20 μM PLP, 0.2 mM NADH, 2 μM LDH, 1.5 μM CBL, 0.1–20 mM L-Ser (or 1–50 mM L-OAS) and 0.05–10 mM L-Hcys. The assay buffers were 50 mM Hepes pH 7.0, 7.5 and 8.0 or sodium phosphate pH 8.0 and 8.5 or 50 mM MOPS, 50 mM bicine, 50 mM proline (MBP) pH 8.5 and 9.0. The reaction was triggered by the addition of 0.5–2 μM *Tg*CBS variants and the oxidation of NADH was monitored at 340 nm.[22] Since L-Ser and L-OAS work as inferior CBL substrates compared to CBS-generated L-Cth,[15,22,23] a background rate was collected for each sample before starting the reaction by the addition of CBL.

The production of H_2S was determined following the formation of lead sulfide at $\lambda = 390$ nm ($\varepsilon_{390} = 5500\ M^{-1}\ cm^{-1}$) upon the reaction of H_2S with lead acetate, as described in.[10,21]

Steady-state kinetic studies were performed using the dimeric fraction of the enzyme isolated by gel filtration.

2.5 | Structural analysis

The structural analysis and graphical representation of *Tg*CBS were performed with Pymol.[24] L-OAS was modeled by superimposing *Tg*CBS with the equivalent region of the structurally related *O*-acetylserine sulfhydrylase (OASS) enzyme from *Haemophilus influenzae* in complex with prereactive L-OAS. The structures of target proteins were obtained from the PDB Database (http://www.rcsb.org) (PDB IDs: 6XWL [*Tg*CBS]; 6Z3S [*Tg*CBS soaked with L-OAS]; 4ZU6 [*Haemophilus influenzae* OASS]). Protein structure predictions were performed with AlphaFold 2.3.0[25] using an adapted version of the AlphaFold code (https://github.com/deepmind/alphafold).

3 | RESULTS

A global overview of the primary structure of CBSs and OCBSs from different organisms with an eye toward highlighting key residues that have been assumed to govern L-Ser/L-OAS substrate specificity is presented in Figure 2. The multiple alignment pointed out the presence of the proposed active site fingerprint residues Ser, Tyr, and Tyr at positions 82, 158, and 248 (residue number according to yeast CBS) in all conventional CBSs, except for CBS from *M. tuberculosis* where a Glu was found at position 248. On the other hand, Ala74, Phe147, and Val226 were found in OCBSs (residue number according to *Hp*CBS). Of note, divergences are present in the case of Val226 of some OCBSs, where Leu was also found.

To examine the validity of fingerprint residues hypothesis, three single mutant enzymes of *Tg*CBS, in which Ser84 is replaced by Ala (S84A), Tyr160 by Phe (Y160F), and Tyr246 by Val (Y246V), and one triple mutant in which Ser84, Tyr160 and Tyr246 are replaced by Ala, Phe and Val, respectively (S84A/Y160F/Y246V) were constructed. All four mutant enzymes were purified as for the wild-type enzyme and showed a single main band on the SDS-PAGE gel with molecular weight identical to wild-type *Tg*CBS (Figure S2). Structural integrity of the mutants was then analyzed by absorbance and far-UV CD spectroscopy (Figure S3A,B). The spectroscopic behavior of all variants closely resembled that of the wild-type in both the absorbance (peak at 410 nm typical of the internal aldimine, Figure S3A) and CD (content of secondary structure elements) spectra (Figure S3B), suggesting no global protein conformational changes. Moreover, the mutations did not change the thermal stability (Figure S3C and Table S2) or oligomeric state of the mutant enzymes. All the variants exist mainly as dimers in solution with a small portion of tetramer as for wild-type *Tg*CBS (Figure S3D).

3.1 | Effects of amino acid substitutions on L-Cth production

In a first approach to investigate the impact of amino acid substitutions on the ability of *Tg*CBS to process L-Ser or L-OAS, we applied

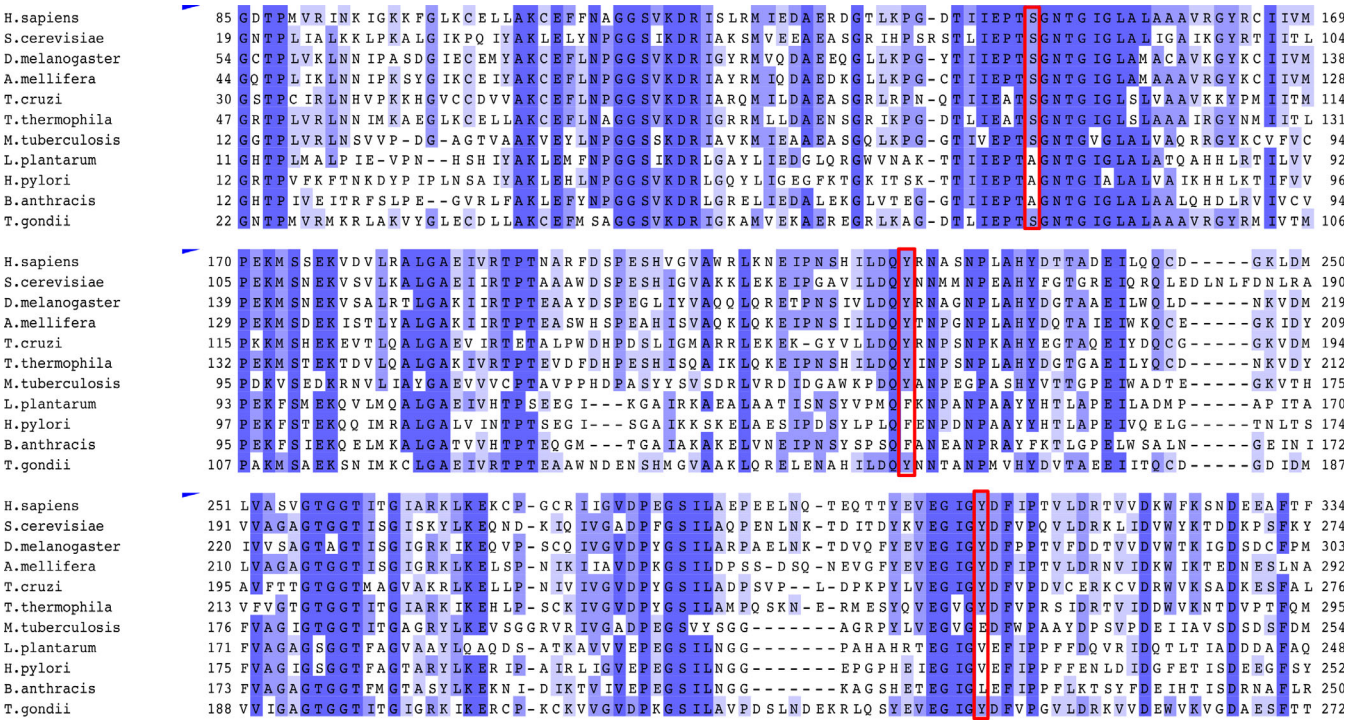

FIGURE 2 Sequence analysis. Multiple alignments of CBSs and OCBSs from different organisms. Red boxes indicate the fingerprint residues that have been assumed to govern L-Ser/L-OAS substrate specificity. A darker color indicates a higher conservation index of the residue. The alignment was obtained with Jalview.[31] *Homo sapiens* (UniProt: P35520); *Saccharomyces cerevisiae* (UniProt: P32582); *Drosophila melanogaster* (UniProt: Q9VRD9); *Apis mellifera* (UniProt: Q2V0C9); *Trypanosoma cruzi* (UniProt: Q9BH24); *Tetrahymena thermophila* (UniProt: I7M350); *Mycobacterium tuberculosis* (UniProt: P9WP51); *Lactobacillus plantarum* (UniProt: F9UT54); *Helicobacter pylori* (UniProt: P56067); *Bacillus anthracis* (UniProt: A0A6L8PXK0); *Toxoplasma gondii* (UniProt: A0A125YSJ9).

reverse phase HPLC with derivatization using ortho-phthaldialdehyde (OPA). This method is a very useful tool to analyze the products of the *Tg*CBS-catalyzed reactions in the presence of different substrates. The formation of L-Cth was investigated for the S84A/Y160F/Y246V mutant after 2 h of reaction time with L-Ser or L-OAS (in the presence of L-Hcys) at pH 9, where maximum activity of *Tg*CBS was previously reported.[10] As shown in Figure 3A,B, L-Cth was the only product detected upon incubation of wild-type *Tg*CBS with L-Ser or L-OAS, confirming that the enzyme is proficient at catalyzing the β-replacement reaction of the two substrates. Notably, no detectable L-Cth product was seen when the triple mutant was incubated with L-Ser (Figure 3A), indicating that the protein variant failed to process L-Ser (as confirmed by the high fluorescence intensity of the unreacted L-Ser substrate). On the other hand, the S84A/Y160F/Y246V mutant was able to produce L-Cth upon incubation with L-OAS (Figure 3B).

Since OCBSs usually possess a shifted optimal pH toward more neutral values (pH ∼ 7.5–8) compared to conventional CBS (pH ∼ 8.5–9), we next performed HPLC at different pH between 7 and 9.5. We found that the pH optimum of the triple variant was decreased by ∼1 pH unit (from 9 to 8) for L-OAS β-replacement activity (Figure 3C), resembling that of OCBSs. No significant product was detected with L-Ser at any pH value tested in agreement with the supposed inability of the triple variant to process L-Ser.

3.2 | Steady-state characterization

To validate the functional meaning of our HPLC observations that the triple mutant exclusively works in the presence of L-OAS without any functionality with L-Ser, we estimated the steady-state kinetics for the triple variant using a CBL-LDH coupled-coupled assay.[22] Initially, the assay was performed from pH 7 to 9.5 and confirmed that the S84A/Y160F/Y246V mutant has optimal activity for the condensation of L-OAS and L-Hcys at pH 8 (Figure 4A), in agreement with HPLC data (Figure 3C). Thus, pH 8 was used for further S84A/Y160F/Y246V mutant enzymatic characterization. Figure 4B shows enzyme kinetics assays for the triple mutant, while Table 1 summarizes the parameters determined. The triple mutation led to a small decrease in k_{cat} for L-OAS (∼1.6-fold) compared to the wild-type enzyme, while no significant differences were observed for K_m. On the other hand, the triple mutant reduced enzyme activity toward L-Ser below the level that could be detected by our assay.

To investigate the individual residue contribution to the enzyme substrate preference, we next analyzed the behavior of each mutation in *Tg*CBS. We found that in the presence of L-Ser, the S84A and Y160F mutations do not affect the optimal pH of the enzyme (pH optimum ∼8.5) (Figure S4A). Interestingly, the Y246V mutation significantly impaired the enzyme's ability to process L-Ser at all pH values. On the other hand, in the case of L-OAS, all the single variants, including Y246V, showed an optimal pH that was shifted to ∼8 (Figure S4B).

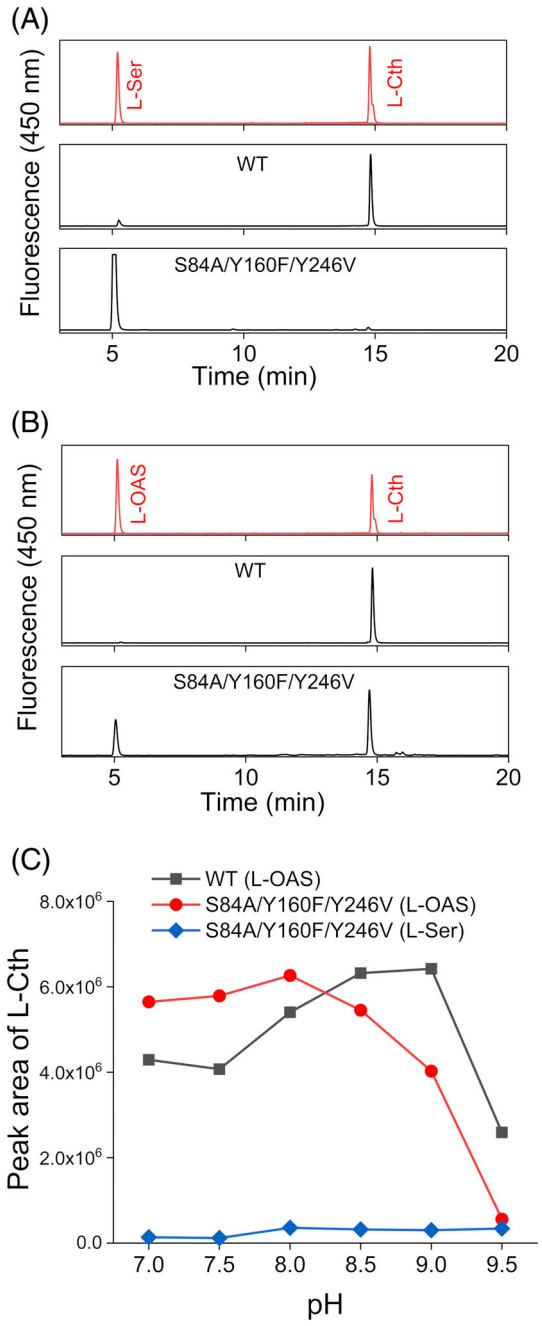

FIGURE 3 Analysis of L-Cth product using reverse phase HPLC. (A) Pure standard L-Ser and L-Cth (top), and product obtained following a 2 h incubation of *Tg*CBS wild-type and its triple variant with 1 mM L-Ser and 0.8 mM L-Hcys. (B) Pure standard L-OAS and L-Cth (top) and product obtained following a 2 h incubation of *Tg*CBS wild-type and its triple variant with 1 mM L-OAS and 0.8 mM L-Hcys. (C) Effect of pH on L-Cth production. The peak areas of L-Cth product detected by HPLC (representative values) were plotted against pH.

Enzymatic assays performed at the specific optimal pH for each variant (Table 1) showed that, similar to the triple mutant, Y246V has severely reduced activity with L-Ser (below the detection level of our coupled assay), suggesting a crucial role of the hydroxyl group of

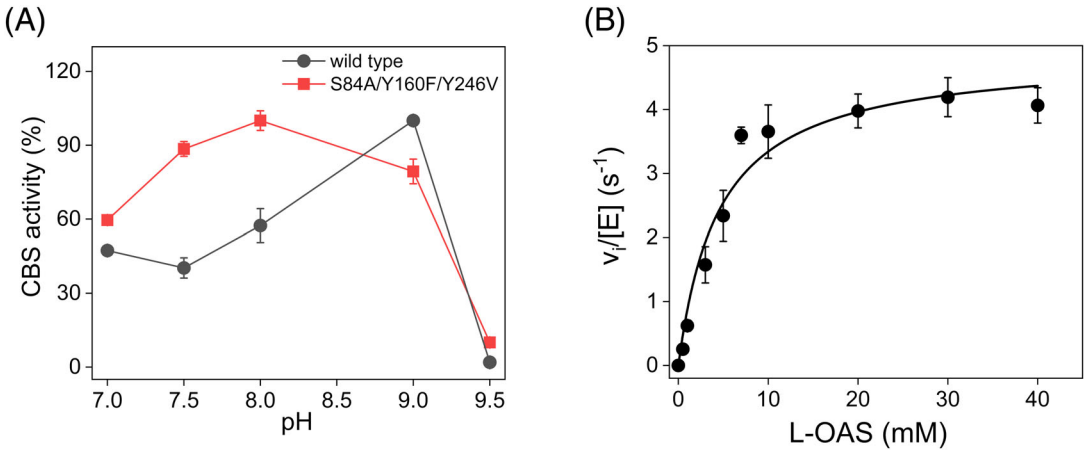

FIGURE 4 Steady state characterization of S84A/Y160F/Y246V mutant. (A) Effect of pH on L-Cth production using L-OAS and L-Hcys as substrates. (B) Steady-state initial velocity kinetics for S84A/Y160F/Y246V variant for the canonical L-OAS + L-Hcys condensation.

TABLE 1 Steady-state kinetic parameters for *Tg*CBS variants[a] at optimal pH.

Protein	Substrate	k_{cat} (s^{-1})	K_m (mM)	k_{cat}/K_m (mM^{-1} s^{-1})
L-OAS + L-Hcys ⟶ L-Cth + acetate				
WT[b]	L-OAS	7.5 ± 0.3	5.1 ± 0.4	1.5 ± 0.2
S84A/Y160F/Y246V[c]	L-OAS	4.7 ± 0.4	4.6 ± 0.5	1.0 ± 0.2
Y246V[c]	L-OAS	6.3 ± 0.3	2.0 ± 0.2	3.2 ± 0.5
Y160F[c]	L-OAS	3.1 ± 0.3	6.9 ± 0.5	0.5 ± 0.1
S84A[c]	L-OAS	1.8 ± 0.2	10.1 ± 0.6	0.20 ± 0.03
L-Ser + L-Hcys ⟶ L-Cth + H_2O				
WT[b]	L-Ser	6.4 ± 0.3	0.7 ± 0.1	9.1 ± 1.7
S84A/Y160F/Y246V[e]	L-Ser	n.d.[d]	n.d.[d]	n.d.[d]
Y246V[e]	L-Ser	n.d.[d]	n.d.[d]	n.d.[d]
Y160F[e]	L-Ser	3.7 ± 0.2	3.8 ± 0.2	1.0 ± 0.1
S84A[e]	L-Ser	0.9 ± 0.2	9.6 ± 0.5	0.10 ± 0.03

Note: Each result shown is the mean ± *SE* of three ($n = 3$) independent experiments.
[a]CBS activity utilizing L-OAS and L-Hcys was determined using CBL from *E. coli* and commercial LDH coupled-coupled assay as in.[22]
[b]Kinetic measurements for the wild-type *Tg*CBS were carried out at pH 9.
[c]Kinetic measurements for all *Tg*CBS mutants in the presence of L-OAS were carried out at pH 8.
[d]n.d. denotes that activity was not detectable.
[e]Kinetic measurements for all *Tg*CBS mutants in the presence of L-Ser were carried out at pH 8.5.

Y246 residue in L-Ser processing. On the other hand, the same mutation did not affect the ability of the enzyme to use L-OAS (Table 1).

The HPLC data for all the variants showed very good agreement with the kinetic profiles obtained (Figure 5) and no L-Cth product was observed for Y246V mutant upon reaction with L-Ser.

Sequence alignment of *Tg*CBS with other CBSs/OCBSs (Figure 2) showed that CBS from *M. tuberculosis* (*Mt*CBS) contains Glu at position 246, whereas other CBSs and OCBSs include Tyr and Val, respectively. Interestingly, *Mt*CBS was recently shown to strictly use L-Ser over L-OAS.[26] Based on this information and to investigate whether Glu at position 246 can determine the selection of L-Ser in *Tg*CBS, we generated also the mutant Y246E. The analysis of the steady-state kinetics (Figure S5A) clearly showed that the Y246E mutation significantly impaired the enzyme's ability to process L-Ser at all pH values, while it only slightly affects the ability of the enzyme to use L-OAS for which optimal pH was shifted to ~8. The HPLC data agree with the kinetic results; very low L-Cth product was observed for Y246E mutant upon reaction with L-Ser (Figure S5B), while the peak corresponding to L-Cth was evident upon incubation of Y246E with L-OAS (Figure S5C). Thus, the effects of Tyr substitution with Glu resemble those of Tyr substitution with Val, confirming the crucial role of the hydroxyl group of Y246 in *Tg*CBS L-Ser processing.

The enzymatic ability of the *Tg*CBS variants to produce H_2S in the presence of L-Cys and L-Hcys was also analyzed. Interestingly, we found no significant differences in the H_2S generating abilities between wild-type and mutant enzymes (Figure S6), indicating that the S84, Y160, and Y246 residues are not crucial for this H_2S alternative reaction and therefore suggesting that the canonical and alternative H_2S-generating activities could be disconnected in *Tg*CBS.

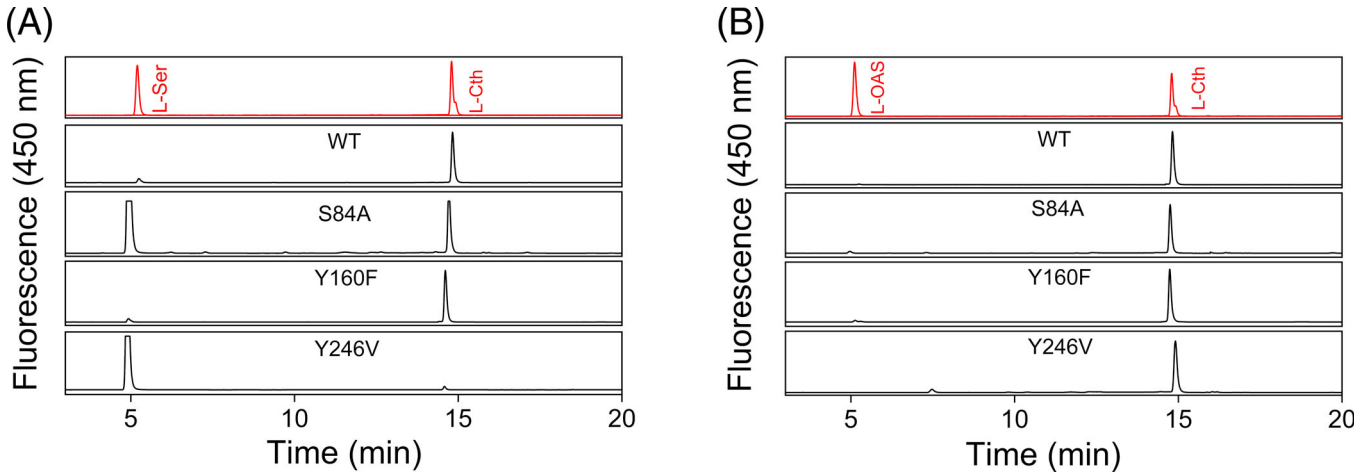

FIGURE 5 Analysis of L-Cth production for *Tg*CBS single mutants using reverse phase HPLC. (A) Pure standard L-Ser and L-Cth (top), and product obtained following a 2 h incubation of *Tg*CBS single variants with 1 mM L-Ser and 0.8 mM L-Hcys. (B) Pure standard L-OAS and L-Cth (top) and product obtained following a 2 h incubation of *Tg*CBS single variants with 1 mM L-OAS and 0.8 mM L-Hcys. The profile of wild-type *Tg*CBS was added for comparison. The analysis was performed at the optimal pH for each variant.

3.3 | Spectroscopic study of catalytic intermediates

CD spectroscopy is a useful technique to readily monitor the reaction intermediates of CBS in the presence of its substrates L-Ser (or L-OAS) and L-Hcys. Thus, we used CD spectroscopy to check whether the loss of activity in the triple and Y246V mutants with L-Ser was because of an alteration in the forward half-reaction with L-Ser or in its complex with L-Hcys. We previously showed that the CD spectrum of wild-type *Tg*CBS exhibited a peak at 410 nm, which corresponds to the internal aldimine (ketoenamine tautomer), formed between the cofactor PLP and the catalytic K56 residue.[10] Addition of either L-Ser or L-OAS to *Tg*CBS leads to the formation of the aminoacrylate, which possesses a negative CD band at 460 nm (Figure 6A,B).[10] Addition of L-Hcys to the aminoacrylate-L-Ser (or L-OAS) complex results in CD spectra that are essentially identical to those of *Tg*CBS alone, indicating the release of the L-Cth and the regeneration of the internal aldimine of the free enzyme.

Notably, when the behavior of the single mutants was analyzed in the same conditions, they were able to promote the formation of the aminoacrylate following the addition of either L-Ser or L-OAS (Figure 6). These data suggest that the punctual substitution of any of the three residues (S84, Y160, and Y246) by a nonpolar amino acid of equivalent size is not a sufficient condition to impair the first step of the ping-pong β-replacement reaction. Of note, the S84A and Y160F variants were able to catalytically progress through the second reaction step to the formation of the final product, L-Cth, upon addition of the second substrate (L-Hcys) to the enzyme-aminoacrylate intermediate formed in the presence of either L-Ser or L-OAS (Figure 6C–F). On the other hand, the Y246V mutant did not spectroscopically recover the 410 nm band characteristic of the internal aldimine upon addition of L-Hcys to the enzyme-aminoacrylate-L-Ser complex, while it did upon addition of L-Hcys to the enzyme-aminoacrylate-L-OAS complex (Figure 6G,H). Therefore, the inability of the variant Y246V to yield L-Cth using L-Ser appears to affect the second step of the reaction.

Of note, the S84A/Y160F/Y246V mutant was able to produce the aminoacrylate intermediate and the final L-Cth product upon incubation with L-OAS and L-Hcys, while no aminoacrylate formation was observed upon reaction with L-Ser (Figure 6I,L).

4 | DISCUSSION

The understanding of the structure–function relationships and the factors underlying specificity in bacterial and parasite CBS enzymes can provide the framework for the design of antimicrobial compounds.

Canonical CBS prefers L-Ser as its first substrate to conduct β-replacement reaction, whereas bacterial OAS-dependent CBS (OCBS) essentially utilizes L-OAS for the reaction and shows no activity toward L-Ser.[1,6,8,9,26,27] CBS from *T. gondii* provides a particularly valuable model for exploring the enzyme-substrate specificity because it similarly processes both L-Ser and L-OAS for β-replacement activity to produce L-Cth.[10–12]

Our analysis of a representative group of 11 prokaryotic and eukaryotic CBSs and OCBSs, for which substrate preference is known, revealed that the polar residues Ser82, Tyr158, and Tyr248 (numbered according to the conventional yeast CBS) are conserved among canonical CBS sequences, while distinct hydrophobic residues (Ala, Phe, and Val) are usually found in OCBSs. Considering the proposal of Devi *et al*, this provides indirect support that these positions play critical roles in defining the L-Ser/L-OAS preference of the two proteins.[8] Since these residues are located close to the active site and help define its architecture, roles in substrate binding have been suggested.[8]

Mutants of *Tg*CBS (S84A, Y160F, Y246V, and S84A/Y160F/Y246V) were generated to explore the roles of the parent amino acids

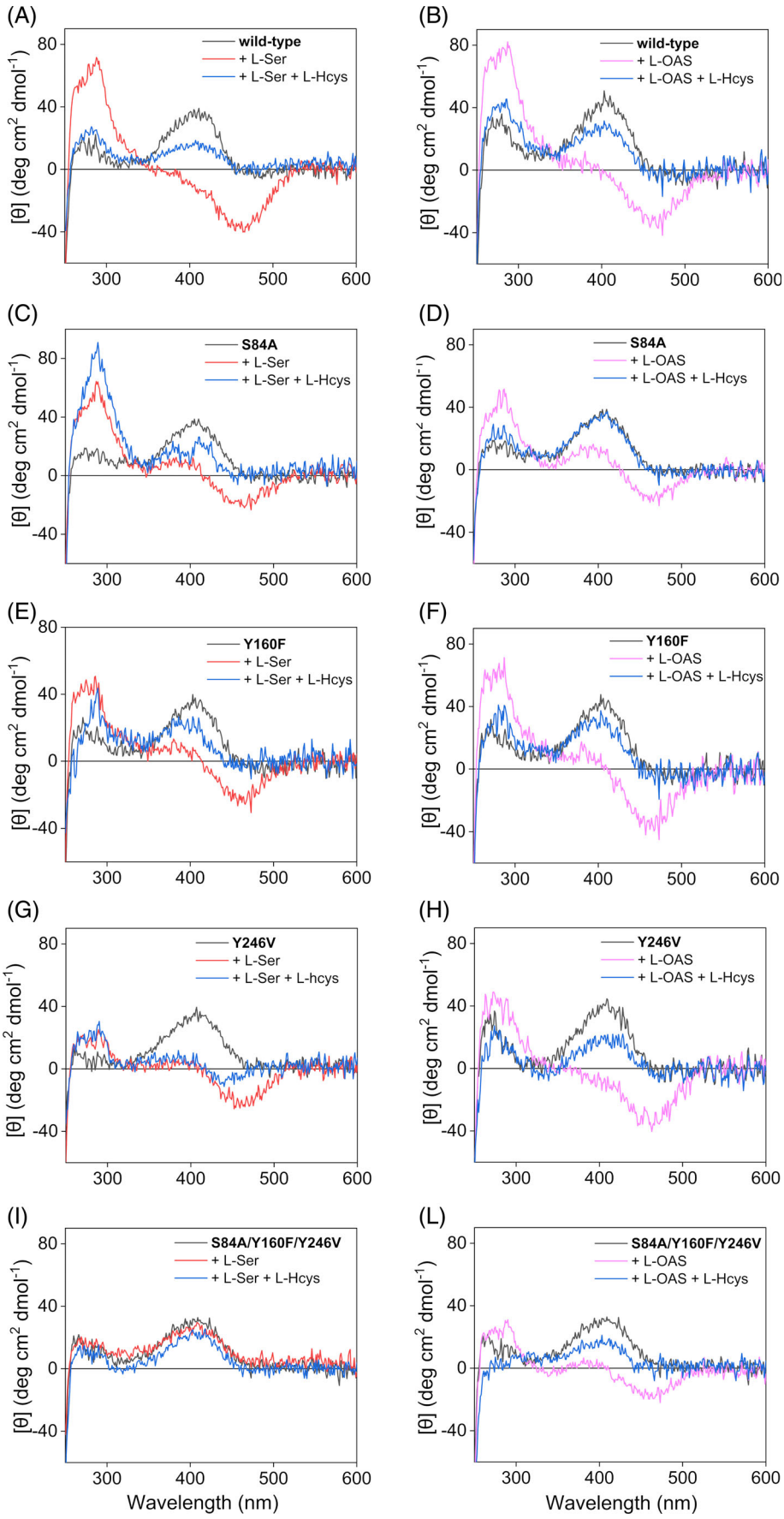

FIGURE 6 CD spectra of wild-type *Tg*CBS and its variants in the presence of L-Ser or L-OAS. Near-UV CD spectra of 1 mg/mL protein variant upon addition of 20 mM L-Ser (A, C, E, G, I) or 20 mM L-OAS (B, D, F, H, L) and 10 mM L-Hcys.

in the L-Ser/L-OAS specificity of the enzyme. The results show that the triple mutation (S84A/Y160F/Y246V) suppresses the L-Ser β-replacement activity of *Tg*CBS, while it does not affect L-OAS binding and processing. Along with this, the triple mutation affects the optimal pH for *Tg*CBS activity toward L-OAS, which is decreased by ~1 pH unit. Although CBSs and OCBSs have a similar structure and share many residues in the active-site, the pH optima for the CBS-catalyzed β-replacement of L-Ser (8.5–9.5) are different from the 7–8 range for the β-replacement of L-OAS catalyzed by OCBSs. The reduction in the catalytic efficiency of OCBSs at higher pH may constitute an evolutionary tradeoff within bacterial OCBS and eukaryotic CBSs. The group responsible for this difference may be the amino group of the substrate. It is possible that the pK_a of this group in L-Ser and L-OAS is influenced by the different active-site environments of CBS and OCBS.[22,28]

Analysis of the independent or combined effect of each mutation in catalytic cavity, by combining the predictive accuracy of AlphaFold-2[25] with the crystal structure of the native enzyme solved by our group,[12] allowed us to conclude that, despite the variation in steric hindrance and reduction of polarity within the cavity caused by the lack of the hydroxyl groups in the substituted side chains, the catalytic site remained basically unaltered when mutations were introduced in the protein sequence.

The initial orientation of L-Ser and L-OAS within the catalytic cavity could be easily modeled based on the orientation of the aminoacrylate molecule found in the *Tg*CBS crystals grown in the presence of L-Ser or L-OAS and coincided with that formerly found in the structurally related *O*-acetylserine sulfhydrylase enzyme from *Haemophilus influenzae* in complex with prereactive L-OAS (PDB ID 4ZU6) (Figures 7 and S7). Interestingly, the aminoacrylate molecule isolated in crystals grown with L-Ser or L-OAS orients its double C—C bond toward the hydroxyl groups of residues S84, Y160, and Y246, which suggests the formation of H-bonds with the hydroxyl group of L-Ser, or alternatively the oxygen of acetyl from OAS, when the substrates enter the cavity. Importantly, these stabilizing interactions favor the release of a water molecule or an acetate group during the first step of the ping-pong reaction. The protein-aminoacrylate complex structure suggests that residue Y246, which is closer to L-Ser and L-OAS than Y160 and S84, is likely the amino acid that most efficiently stabilizes the corresponding leaving groups, although not exclusively, since the Y246V mutation alone is not capable of impairing the formation of the aminoacrylate intermediate. Indeed, as shown in Figure 6, CD spectra clearly detected the aminoacrylate intermediate upon addition of both L-Ser and L-OAS, thus suggesting an incapacitating effect on the second reaction step, either caused by an impaired access or an improper orientation of L-Hcys within the cavity, or by an anomalous release of the L-Cth product that could get trapped inside the cavity. Accordingly, mutating Y246 to Val completely abolished the activity of *Tg*CBS for the substrate L-Ser, suggesting that the hydroxyl moiety of Y246 is critical in L-Ser

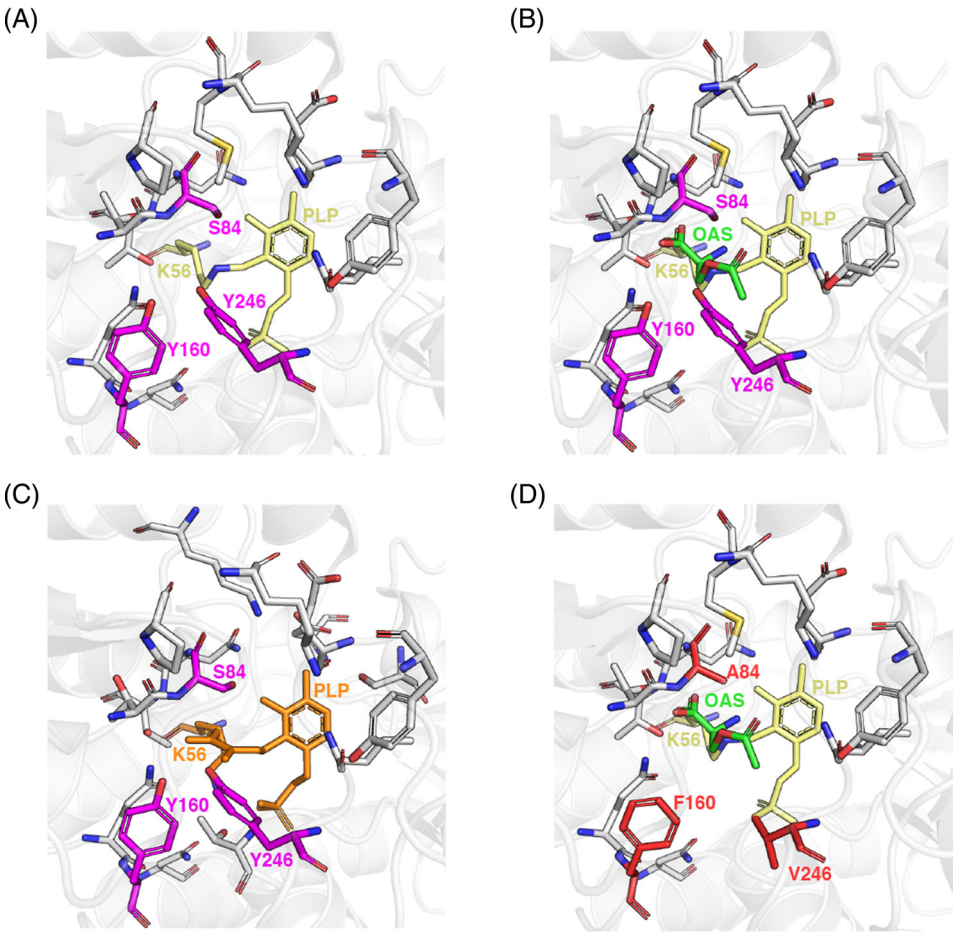

FIGURE 7 Overview of the *Tg*CBS catalytic site. (A) Main amino acid residues configuring the catalytic site of native *Tg*CBS. The coordinates are extracted from the crystal structure of the native enzyme (PDB:6XWL).[12] The three residues S84, Y160 and Y246 are shown in magenta, while the catalytic K56 residue and the PLP are shown in pale yellow. (B) Location of L-OAS (green) within the *Tg*CBS catalytic site, modeled by superimposing *Tg*CBS with the equivalent region of the structurally related *O*-acetylserine sulfhydrylase from *Haemophilus influenzae* in complex with prereactive L-OAS (PDB ID 4ZU6). (C) Location of the aminoacrylate intermediate (orange) observed in crystals of *Tg*CBS grown in the presence of L-Ser or L-OAS.[12] (D) Modeled location of L-OAS within the catalytic cavity of the triple S84A/Y160F/Y246V *Tg*CBS mutant, following the modeling procedure mentioned in panel B.

catalysis. The near-wild type kinetic parameters for L-Ser β-replacement of the Phe variant of Y160 suggest that the hydrogen-bonding moieties of the side chain of this residue do not have a direct role in substrate binding. The residue may participate in substrate positioning or architecture of active site to subtly affect reaction specificity. On the other hand, the reduction of catalytic efficiency values by ~90-fold for the S84A mutant, due to a significant increase in the K_m value compared to wild-type *Tg*CBS, demonstrates that hydroxyl group of Ser84 is also implicated in L-Ser binding and positioning, supporting its importance in the active-site context. However, its punctual substitution by a nonpolar amino acid of equivalent size is not a sufficient condition to impair the β-replacement reaction.

The absence of the aminoacrylate intermediate and consequent inactivation of the S84A/Y160F/Y246V construct upon addition of L-Ser clearly demonstrates that the presence of at least one side-chain hydroxyl group of these residues in the neighborhood of L-Ser is crucial for the binding of L-Ser and is required to perform the first catalytic step. This is not essential in the case of L-OAS, which has a better leaving group (acetate) than L-Ser. As mentioned,[8] it appears that the OH of L-Ser requires the presence of residues containing OH groups in the catalytic site to convert the OH of L-Ser into a good leaving moiety. In the case of L-OAS, the triple mutant lacks OH groups but contains hydrophobic side chains that may interact and stabilize the methyl group of the acetyl moiety, thus debilitating the O—C bond of L-OAS and converting the acetyl into a good leaving group.

Overall, our study has highlighted a crucial role for S84, Y160, and Y246 in selective binding to the physiological substrates L-Ser and L-OAS and affecting the pH optimum of *Tg*CBS. These results increase our understanding of the intricate factors controlling substrate preference in CBSs that are the basis for the design of therapeutics, comprising antimicrobial compounds and modulators of H_2S production, and demonstrate that differences in substrate specificity of CBSs are controlled by natural variations in as few as three residue positions.[23,28–30] Given the central role of CBS in redox cellular homeostasis and cysteine metabolism, it is not surprising that certain residues and structural features in different organisms have evolved to regulate specificity. It is likely that CBSs and OCBSs adapted to dissimilar physiological conditions, in which two substrates have diverse relative concentrations. The functional significance of maintaining β-replacement of both L-Ser and L-OAS in *Tg*CBS is unknown, but it may give a selective advantage for the survivability of the pathogen within its hosts.

AUTHOR CONTRIBUTIONS

Carolina Conter: Investigation; conceptualization; writing – review and editing. **Filippo Favretto:** Writing – review and editing; investigation. **Paola Dominici:** Funding acquisition; writing – review and editing. **Luis Alfonso Martinez-Cruz:** Funding acquisition; writing – review and editing; investigation. **Alessandra Astegno:** Funding acquisition; conceptualization; writing – original draft; writing – review and editing; supervision.

ACKNOWLEDGMENTS

This research was supported by departmental funds provided by the Italian Minister of University and Research (FUR2022) to AA and PD, and in part by the Italian MIUR-PRIN 2017 grant no. 2017ZBBYNC to AA. We thank the Centro Piattaforme Tecnologiche of the University of Verona for providing access to the spectroscopic platform. We also thank MCIN/AEI/10.13039/501100011033 (PID2019-109055RB-I00, CEX2021-001136-S) to LAM-C and CIC bioGUNE.

CONFLICT OF INTEREST STATEMENT

The authors have no conflict of interest to declare.

DATA AVAILABILITY STATEMENT

The data that support the findings of this study are available from the corresponding author upon reasonable request.

ORCID

Carolina Conter https://orcid.org/0000-0002-5999-8667
Alessandra Astegno https://orcid.org/0000-0002-7341-0970

REFERENCES

1. Majtan T, Pey AL, Fernández R, Fernández JA, Martínez-Cruz LA, Kraus JP. Domain organization, catalysis and regulation of eukaryotic cystathionine beta-synthases. *PLOS One*. 2014;9(8):e105290.
2. Ereño-Orbea J, Majtan T, Oyenarte I, Kraus JP, Martínez-Cruz LA. Structural basis of regulation and oligomerization of human cystathionine beta-synthase, the central enzyme of transsulfuration. *Proc Natl Acad Sci U S A*. 2013;110(40):E3790-E3799.
3. Bateman A. The structure of a domain common to archaebacteria and the homocystinuria disease protein. *Trends Biochem Sci*. 1997;22(1):12-13.
4. Baykov AA, Tuominen HK, Lahti R. The CBS domain: a protein module with an emerging prominent role in regulation. *ACS Chem Biol*. 2011;6(11):1156-1163.
5. Anashkin VA, Baykov AA, Lahti R. Enzymes regulated via cystathionine β-synthase domains. *Biochemistry (Moscow)*. 2017;82(10):1079-1087.
6. Koutmos M, Kabil O, Smith JL, Banerjee R. Structural basis for substrate activation and regulation by cystathionine beta-synthase (CBS) domains in cystathionine β-synthase. *Proc Natl Acad Sci*. 2010;107(49):20958-20963.
7. Giménez-Mascarell P, Majtan T, Oyenarte I, et al. Crystal structure of cystathionine β-synthase from honeybee *Apis mellifera*. *J Struct Biol*. 2018;202(1):82-93.
8. Devi S, Tarique KF, Ali MF, Abdul Rehman SA, Gourinath S. Identification and characterization of *Helicobacter pylori O*-acetylserine-dependent cystathionine β-synthase, a distinct member of the PLP-II family. *Mol Microbiol*. 2019;112(2):718-739.
9. Devi S, Abdul Rehman SA, Tarique KF, Gourinath S. Structural characterization and functional analysis of cystathionine beta-synthase: an enzyme involved in the reverse transsulfuration pathway of *Bacillus anthracis*. *FEBS J*. 2017;284(22):3862-3880.
10. Conter C, Fruncillo S, Fernández-Rodríguez C, Martínez-Cruz LA, Dominici P, Astegno A. Cystathionine β-synthase is involved in cysteine biosynthesis and H(2)S generation in *Toxoplasma gondii*. *Sci Rep*. 2020;10(1):14657.
11. Conter C, Fruncillo S, Favretto F, et al. Insights into domain organization and regulatory mechanism of cystathionine beta-synthase from *Toxoplasma gondii*. *Int J Mol Sci*. 2022;23(15):8169.
12. Fernández-Rodríguez C, Oyenarte I, Conter C, et al. Structural insight into the unique conformation of cystathionine β-synthase from *Toxoplasma gondii*. *Comput Struct Biotechnol J*. 2021;19:3542-3555.
13. Gut H, Dominici P, Pilati S, et al. A common structural basis for pH- and calmodulin-mediated regulation in plant glutamate decarboxylase. *J Mol Biol*. 2009;392(2):334-351.

14. Astegno A, Capitani G, Dominici P. Functional roles of the hexamer organization of plant glutamate decarboxylase. *Biochim Biophys Acta*. 2015;1854(9):1229-1237.
15. Allegrini A, Astegno A, la Verde V, Dominici P. Characterization of C-S lyase from *Lactobacillus delbrueckii* subsp. *bulgaricus* ATCC BAA-365 and its potential role in food flavour applications. *J Biochem*. 2017;161(4):349-360.
16. Astegno A, Bonza MC, Vallone R, et al. *Arabidopsis* calmodulin-like protein CML36 is a calcium (Ca^{2+}) sensor that interacts with the plasma membrane Ca^{2+}-ATPase isoform ACA8 and stimulates its activity. *J Biol Chem*. 2017;292(36):15049-15061.
17. Spyrakis F, Faggiano S, Abbruzzetti S, et al. Histidine E7 dynamics modulates ligand exchange between distal pocket and solvent in AHb1 from *Arabidopsis thaliana*. *J Phys Chem B*. 2011;115(14):4138-4146.
18. Maresi E, Janson G, Fruncillo S, et al. Functional characterization and structure-guided mutational analysis of the transsulfuration enzyme cystathionine γ-lyase from *Toxoplasma gondii*. *Int J Mol Sci*. 2018;19(7):2111.
19. Astegno A, Maresi E, Bertoldi M, la Verde V, Paiardini A, Dominici P. Unique substrate specificity of ornithine aminotransferase from *Toxoplasma gondii*. *Biochem J*. 2017;474(6):939-955.
20. Conter C, Bombardi L, Pedretti M, et al. The interplay of self-assembly and target binding in centrin 1 from *Toxoplasma gondii*. *Biochem J*. 2021;478(13):2571-2587.
21. Chiku T, Padovani D, Zhu W, Singh S, Vitvitsky V, Banerjee R. H2S biogenesis by human cystathionine gamma-lyase leads to the novel sulfur metabolites lanthionine and homolanthionine and is responsive to the grade of hyperhomocysteinemia. *J Biol Chem*. 2009;284(17):11601-11612.
22. Aitken SM, Kirsch JF. Kinetics of the yeast cystathionine beta-synthase forward and reverse reactions: continuous assays and the equilibrium constant for the reaction. *Biochemistry*. 2003;42(2):571-578.
23. Hopwood EM, Ahmed D, Aitken SM. A role for glutamate-333 of Saccharomyces cerevisiae cystathionine gamma-lyase as a determinant of specificity. *Biochim Biophys Acta*. 2014;1844(2):465-472.
24. DeLano W. *The PyMOL Molecular Graphics System*. DeLano Scientific; 2002.
25. Jumper J, Evans R, Pritzel A, et al. Highly accurate protein structure prediction with AlphaFold. *Nature*. 2021;596(7873):583-589.
26. Bandyopadhyay P, Pramanick I, Biswas R, et al. S-adenosylmethionine-responsive cystathionine β-synthase modulates sulfur metabolism and redox balance in *Mycobacterium tuberculosis*. *Sci Adv*. 2022;8(25):eabo0097.
27. Lv H, Xu J, Bo T, Wang W. Characterization of cystathionine β-synthase TtCbs1 and cysteine synthase TtCsa1 involved in cysteine biosynthesis in Tetrahymena thermophila. *J Eukaryot Microbiol*. 2021;68(2):e12834.
28. Aitken SM, Lodha PH, Morneau DJ. The enzymes of the transsulfuration pathways: active-site characterizations. *Biochim Biophys Acta*. 2011;1814(11):1511-1517.
29. Lodha PH, Jaworski AF, Aitken SM. Characterization of site-directed mutants of residues R58, R59, D116, W340 and R372 in the active site of *E. coli* cystathionine beta-lyase. *Protein Sci*. 2010;19(3):383-391.
30. Lodha PH, Aitken SM. Characterization of the side-chain hydroxyl moieties of residues Y56, Y111, Y238, Y338, and S339 as determinants of specificity in *E. coli* cystathionine beta-lyase. *Biochemistry*. 2011;50(45):9876-9885.
31. Waterhouse AM, Procter JB, Martin DMA, Clamp M, Barton GJ. *Jalview version 2—a multiple sequence alignment editor and analysis workbench*. *Bioinformatics*. 2009;25(9):1189-1191.

SUPPORTING INFORMATION

Additional supporting information can be found online in the Supporting Information section at the end of this article.

How to cite this article: Conter C, Favretto F, Dominici P, Martinez-Cruz LA, Astegno A. Key substrate recognition residues in the active site of cystathionine beta-synthase from *Toxoplasma gondii*. *Proteins*. 2023;91(10):1383-1393. doi:10.1002/prot.26507